Journal of Nuclear Medicine, published on May 30, 2019 as doi:10.2967/jnumed.119.226787

Imaging chemotherapy induced acute cardiotoxicity with ^{18}F-labelled lipophilic cations

Authors: Stuart P McCluskey,[1,2] Anna Haslop,[1] Christopher Coello,[2] Roger N Gunn,[2,3] Edward W Tate,[1] Richard Southworth,[4] Christophe Plisson,[2] Nicholas J Long,*[1] Lisa A Wells,*[2]

Author affiliations: 1. Department of Chemistry, Imperial College London, 2. Invicro LLC., 3. Division of Brain Sciences, Imperial College London, Imperial College Centre for Drug Discovery Science, 4. Biomedical Engineering and Imaging Sciences, King's College London

*Corresponding Author*s: Professor Nicholas Long, Imperial College London, MSRH, White City Campus, London W12 0BZ, (0)2075945781, n.long@imperial.ac.uk; Dr Lisa Wells, Invicro LLC., Burlington Danes Building, Hammersmith Hospital, Du Cane Road, London, W120NN, (0)2080086000, lisa.wells@invicro.co.uk

Lead Author: Dr Stuart McCluskey, Imperial College London, MSRH, White City Campus, London W12 0BZ, +447507456976, s.mccluskey13@imperial.ac.uk

Wordcount: 5148

Running title: Imaging acute doxorubicin cardiotoxicity

Abstract

Many chemotherapy agents are toxic to the heart, such that increasing numbers of cancer survivors are now living with the potentially lethal cardiovascular consequences of their treatment. Earlier and more sensitive detection of chemotherapy-induced cardiotoxicity may allow improved treatment strategies and increase long-term survival. Lipophilic cation positron emission tomography (PET) tracers may be suitable for early detection of cardiotoxicity. This study aims to evaluate an ^{18}F-labelled lipophilic phosphonium cation e.g. ^{18}F-Mitophos, as a cardiac imaging agent, comparing it to leading PET and SPECT lipophilic cationic tracers before further assessing its potential for imaging cardiotoxicity in an acute doxorubicin (DOX) model.

Methods

Cardiac uptake and response to decreased mitochondrial membrane potential ($\Delta\Psi_m$) of ^{18}F-Mitophos and ^{99m}Tc-Sestamibi were tested in isolated perfused rat hearts. Baseline pharmacokinetic profiles of ^{18}F-Mitophos and ^{18}F-FBnTP and their response to acute DOX-induced cardiotoxicity were assessed in rats *in vivo* (10, 15 or 20 mg/kg DOX, *i.v.*, 48 h prior).

Results

Cardiac retention of ^{18}F-Mitophos was over double that of ^{99m}Tc-Sestamibi in isolated perfused rat hearts. Favourable biodistribution of ^{18}F-Mitophos *in vivo* was observed with heart to tissue ratios of 304 ± 186, 11.2 ± 1.2 and 3.8 ± 0.6 for plasma, liver and lung respectively (60 min). A significant dose-dependent loss of cardiac retention of ^{18}F-Mitophos was observed upon DOX treatment where average cardiac $SUV_{30\text{-}60}$ (mean ± SD) decreased from 3.5 ± 0.5 (control) to 1.8 ± 0.1 (DOX 20 mg/kg). Other biomarkers assessed showed no alterations.

Conclusions

^{18}F-Mitophos showed suitable pharmacokinetic parameters for cardiac imaging. A significant dose-response of cardiac uptake to DOX treatment was observed before detectable biomarker alterations. It is therefore, a promising tracer for imaging chemotherapy-induced cardiotoxicity. This is the first demonstration of PET radiolabelled lipophilic cations being used for the imaging of chemotherapy-induced cardiotoxicity imaging and indicates the potential application of these compounds in this area.

Keywords: Phosphonium cations, 18F radiochemistry, PET, cardiotoxicity, doxorubicin

Introduction

Long term cancer survival rates are increasing, with >5 year survival rate rising from 49% for diagnoses made in the mid-1970s, to 69% for diagnoses made in 2005-2011, in the United States.[1] However, many cancer treatments are not themselves benign, and the long term effects of cancer treatment are increasingly impacting upon patient morbidity and mortality. Doxorubicin (DOX) is a widely used and effective anthracycline chemotherapy agent used in the treatment of a variety of cancers.[2,3] Its therapeutic potential, however, is limited by severe and potentially lethal cardiotoxic effects. Approximately 10% of patients treated with DOX will develop potentially life threatening cardiotoxicity up to 10 years after treatment,[4] with higher cumulative doses increasing risk dramatically.[5] Of those who develop congestive heart failure, mortality is approximately 50%.[6,7]

Cardiotoxicity is currently routinely monitored by echocardiography (echo) or MUGA scanning, typically defined by a greater than 10% reduction of left ventricle ejection fraction (LVEF).[3,8] However, such loss of contractile function typically indicates significant irreversible myocardial injury, where opportunities to intervene or modify treatment are limited.[3,9]

Measuring evolving cardiac damage at a sub-cellular level using a molecular imaging approach could provide earlier and more sensitive assessment of cardiotoxicity, however most approaches explored to date are limited in capacity or in a relatively early stage .[10,11]

'Metabolism' tracers such as ^{18}F-FDG and ^{11}C-acetate have been investigated, however, cardiac retention is heavily influenced by other parameters, such as dietary substrate availability, which complicate their use.[12] Tracers more closely related to the mechanisms of cardiotoxicity such as ^{123}I-MIBG, which is sensitive to sympathetic nervous system alterations, show greater promise and have shown response to DOX treatment pre-clinically, and in patients.[13] However, slow clearance from blood and significant liver uptake impact upon their clinical utility.[14]

Although the exact mechanism of cardiotoxicity by DOX is not fully understood, mitochondrial dysfunction, directly or indirectly, is central to the proposed mechanisms.[4,15,16] Fluorescent lipophilic cations such as the rhodamine or JC-1 dyes have been used to report on mitochondrial function *in vitro* for many years. They accumulate via passive diffusion through cell membranes of mitochondria according to the mitochondrial membrane potential ($\Delta\Psi_m$), with PET-labelled derivatives showing good sensitivity in myocardial infarction models.[17] Our collaborators have recently demonstrated the potential for using radiolabelled lipophilic cations to report on doxorubicin-induced mitochondrial dysfunction with ^{99m}Tc-sestamibi for SPECT imaging.[18] While proof of concept with SPECT imaging has been demonstrated, PET has significant advantages for this approach in terms of sensitivity and the capacity for 3-dimensional pharmacokinetic analysis.

This study therefore aims to evaluate our recently developed PET lipophilic cation ^{18}F-Mitophos[19] as a cardiac imaging agent. We hypothesise that PET radiolabelled lipophilic

cations such as ^{18}F-Mitophos, which are sensitive to $\Delta\Psi_m$ alterations and accumulate in cardiac tissue, may allow early detection of DOX-induced cardiotoxicity, potentially before mechanical alterations in cardiac function manifest.

Materials and Methods

Animal Procedures

All animal procedures were performed in accordance with the United Kingdom Home Office Animals (Scientific Procedures) Act 1986 and the EU directive 2010/63/EU. The procedures were reviewed by independent ethics committees (Imperial College London and King's College London). All animals were sourced from Charles River.

Radiopharmaceutical Preparation

^{18}F-Mitophos was produced in >99% radiochemical purity and molar activity of 24.6 ± 18.3 GBq/μmol by a fully automated two-step radiosynthesis process, adapted from the previously reported methodology (Figure 1).[20] ^{18}F-FBnTP was produced in >99% radiochemical purity and specific activity 15.0 ± 12.6 GBq/μmol in a fully automated four-step radiosynthesis, modified from literature (Figure 1).[21] For further details please refer to Online Supplement. ^{99m}Tc-sestamibi was prepared from commercial cold kits (Mallinckrodt Pharmaceuticals) reconstituted with saline (100 MBq/mL) from a ^{99}Mo/^{99m}Tc generator and supplied by the radiopharmacy at St. Thomas' Hospital, King's College, London, UK.

Langendorff Heart Perfusion

To investigate tracer response to decreased $\Delta\Psi_m$, uptake and kinetic modelling of ^{18}F-Mitophos was compared to that of SPECT lipophilic cardiac tracer ^{99m}Tc-Sestamibi in male Wistar rat hearts (n = 4-6 per group, 300-330 g) on a triple-γ-detection Langendorff perfusion set-up, previously described.[22,23] Tracers were compared under normoxic control perfusion and in hearts treated with the $\Delta\Psi_m$ uncoupler carbonyl cyanide 3-chlorophenylhydrazone (CCCP). Cardiac function of perfused hearts was monitored through measurements of left ventricular end-diastolic pressure (LVEDP) and left ventricular developed pressure (LVDP). Cardiac radiotracer uptake was recorded, decay corrected, and exponential washout component (K) was calculated from least squares fit of data from 2 min post injection.

***Ex vivo* biodistribution**

Male Sprague Dawley rats (300-500 g; n = 3 per time-point) were anaesthetised and ^{18}F-Mitophos or ^{18}F-FBnTP (5.1 ± 1.3 MBq) was administered intravenously (*i.v.*) Animals were culled at 5, 15, 30 or 60 min post administration and tissues were collected and radioactivity measured via gamma counter (Wizard).

The distribution of radioactivity in tissue and plasma are expressed as mean standardised uptake values (SUV), where SUV = (%ID x BW)/100%ID is the percent of injected dose per gram of tissues and BW is the body weight of the animal (g).

Metabolite Analysis

Blood samples were collected 5, 10, 20, 40 and 60 min post tracer administration (n = 3 per timepoint). Proteins were precipitated from plasma with acetonitrile (ACN) (plasma: ACN ration 1:1) and centrifuged. HPLC analysis of supernatant allowed the parent fraction to be determined.

Dynamic PET:CT cardiac scanning

Animals were anaesthetised and venous and arterial angiocatheters were inserted for radiotracer injection and periodic blood sampling, respectively. A CT scan was conducted for attenuation correction before injection of radiotracer and dynamic PET data acquired (60 min). Selected regions of interest were drawn over the heart and used to generate the time activity curves (TACs).

***In vivo* intra-animal variability**

Sprague Dawley rats (n = 4, 408 ± 95 g) underwent 60 min dynamic PET-CT scans with injection of ^{18}F-Mitophos (6.2 ± 2.0 MBq). After 48 h, animals were scanned a second time with ^{18}F-Mitophos (7.2 ± 1.2 MBq). Cardiac $SUV_{30\text{-}60}$ was determined from dynamic scan TAC of the left ventricle and was used to calculate variability.

Acute *in vivo* DOX cardiotoxicity model

Sprague Dawley rats underwent slow continuous *i.v.* infusion of DOX (10, 15 or 20 mg/kg) over 1 h. Rats were monitored for signs of adverse effects over a 48 h period. 48 h post DOX infusion, rats were placed under terminal anaesthesia and ^{18}F-Mitophos (6.3 ± 1.7

MBq) was injected *i.v.* A subset of rats (n = 3 and n = 4 for the 15 mg/kg and 20 mg/kg groups, respectively) underwent dynamic PET-CT scans with TAC generation over left ventricle. Target tissue activity was measured with a gamma counter 60 min post injection; cardiac tissue and blood plasma were frozen for further analysis.

Cardiotoxicity biomarker analysis

Plasma collected at the end of the protocol was analysed for cardiac troponin-I levels (Ultra-sensitive rat cardiac troponin-I ELISA, Life diagnostics, UK). Samples were thawed to ambient temperature and ELISA carried out as per the manufacturer's instructions, with adaptations of the standard curve to increase sensitivity for lower doses. Standard curve from 19.5 pg/mL to 625 pg/mL rat cardiac troponin-I was used for quantification (R^2 >0.999).

Levels of malondialdehyde (MDA) were evaluated in cardiac muscle tissue as a biomarker of oxidative stress. MDA was extracted from left ventricle tissue as previously described.[24] Each sample was transferred to a 96 well plate for reading and measured in triplicate (absorbance, 586 nm). A standard curve from 1.25 to 40 nmol/mL MDA was used for quantification (R^2 >0.999).

Histological assessment of cardiac tissue from DOX treated rats was carried out on longitudinal sections of ventricle via H&E staining. Fresh-frozen cardiac tissue was sectioned (10 μm) using a cryostat and thaw-mounted onto superfrost slides. Staining was carried out by fixing the tissue with Clarkes solution (3:1 v/v EtOH: glacial acetic acid).

Slides were incubated with haematoxylin solution, differentiated in 1% HCl, before submerging in eosin solution (aq. 1%). Tissue was then dehydrated in EtOH (85%, 100%, 100%), cleared in xylene and allowed to dry prior to the application of DPX medium. Myocardial damage (n = 3 sections per heart, n = 4 hearts per group) was assessed by two independent researchers blind to the treatment groups using a similar scoring system reported by Erboga *et al.*[25] Randomly selected cardiac sections were imaged and assessed for signs of myocardial damage, namely myofibrillar loss, cytoplasmic vacuolisation, myocardial disorganisation, inflammatory cell infiltration and haemorrhages with a score of no damage (0), mild (1), moderate (2) and severe (3).

Statistical analysis

Statistical analysis was carried out using an unpaired t-test, one way ANOVA with Dunnett's post hoc analysis or two-way ANOVA with Dunnett's post hoc analysis where appropriate (GraphPad Prism 7 software). All graphs and values are represented as average values ± standard deviation (SD). Differences between datasets were deemed statistically significant when the observed confidence interval, $P<0.05$.

Results

***In vitro* analysis on Langendorff perfused hearts**

Infusion of CCCP (300 nmol/L) into isolated perfused hearts invoked a significant increase in LVEDP, from 6.9 ± 2.3 to 67.5 ± 10.0 mmHg, and significant decrease in LVDP from 122.4 ±11.1 to 37.7 ± 17.1 mmHg vs control experiments, at 65 min post perfusion

(Supplement Figure 1). Cardiac time-activity profiles were measured from the cardiac orientated γ-detector, for both ^{18}F-Mitophos and ^{99m}Tc-Sestamibi (Figure 2 A, B). In control hearts, ^{18}F-Mitophos exhibited an average single pass extraction and retention of 66 ± 5% (n = 5) of injected spike at 20 min post injection in comparison to ^{99m}Tc-Sestamibi which showed 31 ± 4% (n = 5) retention. In control hearts the kinetic washout rate, K, from 2 min post injection for ^{18}F-Mitophos and ^{99m}Tc-Sestamibi was $1.1x10^{-3} \pm 3x10^{-4}$%ID/min and $4.5x10^{-3} \pm 1.0x10^{-3}$%ID/min respectively (Supplement Figure 1). Upon treatment with CCCP both ^{18}F-Mitophos (n = 4) and ^{99m}Tc-Sestamibi (n = 6) showed a significant decrease in retention from 2 min post injection which was maintained throughout (15% and 12% of injected dose respectively by the end of protocol) (Figure 2 A, B). A significant increase in K was observed for both tracers in hearts treated with CCCP (Supplement Figure 2), with relative increase of 469 ± 150% and 395 ± 146% for ^{18}F-Mitophos and ^{99m}Tc-Sestamibi respectively (Figure 2C).

***Ex vivo* Biodistribution of ^{18}F-Mitophos and ^{18}F-FBnTP**

Ex vivo tissue biodistribution and image derived (30-60 min) SUV data for ^{18}F-Mitophos and ^{18}F-FBnTP are shown in Table 1. There was no substantial bone uptake, alongside good metabolic stability of ^{18}F-Mitophos *in vivo*, with 40% of the parent compound still present in plasma at 60 min post injection (Supplement Table 1 and Supplement Figure 3). In accordance with the isolated heart experimental results, fast uptake and high retention of ^{18}F-Mitophos was observed in the myocardium of healthy animals with an average SUV from *ex vivo* biodistribution of 5.40 ± 0.61 at 5 min post injection and 5.17 ± 0.86 at 60 min. Rapid clearance of ^{18}F-Mitophos from the plasma, liver and lungs was observed, with

relative heart to tissue ratios at 60 min of; 303.9 ± 136.0, 11.2 ± 1.2 and 3.8 ± 0.6 respectively. Distinction of the entire myocardium from all surrounding tissues was apparent in PET-derived images. Intra-animal variability data of ^{18}F-Mitophos (Supplement Figure 4) showed good cardiac uptake repeatability with average divergence of image derived cardiac SUV of 8.0 ± 4.3% from baseline scans.

^{18}F-FBnTP showed similar biodistribution to ^{18}F-Mitophos, with higher uptake in the heart (SUV 7.42 ± 0.43 at 5 min via *ex vivo* biodistribution), and rapid clearance from the bloodstream (Table 1) High liver uptake and retention was observed, with consistent heart to liver ratios around 2 throughout the 60 min protocol.

Acute DOX treatment model

Progressive weight loss was observed over the 48 h period for every DOX treatment group with the 15 mg/kg DOX group showing greatest weight loss of 7.0 ± 1.5%. No severe adverse effects, as defined by two or more persistent signs of ill health, or unscheduled deaths, were encountered through the acute experiment (Supplement Table 2). *Ex vivo* tissue biodistribution data supports a significant, dose dependent decrease in cardiac retention at 60 min post ^{18}F-Mitophos injection in all DOX-treated groups with SUV decreased from 5.3 ± 0.9 (control) to 3.4 ± 0.3 (20 mg/kg DOX), $P<0.001$ (Figure 3 A). Strong correlation with cardiac SUV derived from the dynamic scan data (Figure 3 B, Figure 4) was observed, with a decrease in left ventricle cardiac $SUV_{30\text{-}60}$ from 3.5 ± 0.5 in control, to 1.8 ± 0.1, $P<0.001$ for the 20 mg/kg DOX group. Image derived myocardial

TAC's showed significant alteration between control and DOX treated groups for myocardium and lung (Figure 5, Supplement Figure 6). No significant alterations were observed in SUV of liver, kidney, blood or plasma by *ex vivo* biodistribution across treatment groups (Supplement Figure 5).

Biomarker and histological assessment of *in vivo* DOX-induced cardiac damage

Cardiac troponin-I levels in the plasma 48 h post DOX dose were below the limit of detection of the assay (39 pg/mL) for every sample in each treatment group. No significant differences in MDA concentration were detected in cardiac tissue collected at the end of the protocol across all groups (Supplement Figure 7). Histological assessment of cardiac damage showed substantial increase in semi-quantitative damage assessment between treatment groups and DOX treated groups (Table 2). Typical examples of cardiac sections categorised are displayed in Supplement Figure 8.

Discussion

The long term cardiotoxic side effects of chemotherapy treatment are becoming increasingly important as cancer detection and survival rates increase. The current methods for cardiotoxicity monitoring rely on late-stage, structural and/or mechanical cardiac dysfunction, where irreversible damage has already occurred, and the optimal window for intervention past. Research into radiolabelled tracers as potential early identifiers of cardiotoxicity show some potential, but tracers investigated to date have various

limitations. Here, we show that ^{18}F-Mitophos has a favourable pharmacokinetic profile for cardiac imaging and is responsive to DOX induced cardiotoxicity in an acute rodent model.

Historically, radiolabelled lipophilic cations have long been used as myocardial perfusion imaging agents, based on the assumption that their rapid sequestration into cardiac mitochondria is primarily limited by their delivery.[26,27] However, more recently, the repurposing of the approach to report upon mitochondrial membrane potential itself is becoming of interest. A number of recent preclinical imaging studies have investigated the potential of utilising PET radiolabelled lipophilic cation tracers in myocardial infarction models,[17,28,29] as well as for the quantification of cardiotoxicity by SPECT imaging.[18] To directly compare the *in vivo* performance of ^{18}F-Mitophos to another lipophilic cation ^{18}F-FBnTP was chosen as the only PET lipophilic cation agent to be translated into man.

In the Langendorff perfusion heart model, the cardiac retention of ^{18}F-Mitophos in control perfused hearts was over double that of ^{99m}Tc-Sestamibi, with a higher first-pass extraction and four times slower washout rate from 2 min post injection. This indicates that cardiac uptake of ^{18}F-Mitophos *in vivo* will likely be higher than that of ^{99m}Tc-Sestamibi, and retained for longer. Both tracers exhibited significant washout in response to mitochondrial depolarisation with the ionophore CCCP, indicating their potential to report on mitochondrial dysfunction *in vivo*.

Our *in vivo* pharmacokinetic and biodistribution studies confirmed high uptake and stable retention of both ^{18}F-Mitophos and ^{18}F-FBnTP in the myocardium, and efficient washout

from blood. ^{18}F-Mitophos showed efficient washout from the liver with heart to liver ratios >11 by 60 min, whereas for ^{18}F-FBnTP this remained at 2 throughout, in line with previously published studies.[30] Because of the proximity of heart and liver, high hepatic retention can impact on a tracer's usefulness in cardiac imaging with estimations of SUV in the cardiac apex becoming problematic. This is a major issue of many cardiac tracers in human studies, including ^{18}F-FBnTP where ratios are substantially lower than in rodents (<0.2).[31] As such, the rapid clearance from the liver that ^{18}F-Mitophos displays may be a significant advancement over currently used agents, warranting further investigation into its use as a PET cardiac perfusion imaging agent.

In this study, a single acute DOX dose was applied to investigate the ability of ^{18}F-Mitophos to image cardiac tissue damage, and is the first to characterise a PET radiolabelled lipophilic cation for imaging DOX-induced cardiotoxicity. ^{18}F-Mitophos showed a significant, dose-dependent decrease in cardiac uptake in animals treated with DOX, with left ventricular retention decreasing to almost 50% of controls from dynamic scan data. These results were obtained before detectable plasma levels of cardiotoxicity biomarker cardiac troponin-I had accrued, or significant alterations in cardiac MDA occurred.

The lack of biomarker alteration observed in this study is in line with other acute DOX models in the literature. Biomarker alterations are generally observed only after longer timeframes, 72-96 h,[24,32] or with higher DOX doses, over 48 h.[25,33,34] However, in our model histological assessment of cardiac tissue detected an increase in tissue damage. This

indicates that mitochondria or $\Delta\Psi_m$ may be compromised in the early stages of cardiotoxicity, and that changes seen with ^{18}F-Mitophos may allow early detection of cardiotoxicity. Another possibility is a reduction in blood flow due to cardiac atrophy, which has been shown in humans and rodents after prolonged exposure to DOX.[35,36] While we cannot definitively rule this out as a contributor, a similar DOX study showed no response in perfusion tracer ^{99m}Tc-NOET, implying no alteration in perfusion, but observing significant decrease in ^{99m}Tc-Sestamibi (also a lipophilic cation).[18] The lack of comparison to other perfusion tracers is, however, a limitation of the study. While the initial data presented here on ^{18}F-Mitophos show promise, additional studies are required. Chronic models more representative of clinical procedures would allow meaningful comparison to echo techniques and assess clinical translation potential.

In conclusion, we have reported the potential of the radiolabelled lipophilic cation PET tracer ^{18}F-Mitophos for imaging evolving mitochondrial cardiotoxicity. ^{18}F-Mitophos showed improved pharmacokinetic characteristics over clinically used radiolabelled lipophilic cations, for the purposes of cardiac imaging, with fast washout from blood and liver and stable retention in the myocardium. We also reported the significant dose response of ^{18}F-Mitophos cardiac uptake to acute DOX dose 48 h prior. These results show that ^{18}F-Mitophos is a promising agent for imaging DOX induced cardiotoxicity, with potential as an early diagnostic tool. Further studies on ^{18}F-Mitophos in chronic toxicity models are justified from the results outlined within this work.

Disclosures

No disclosures

Acknowledgements

Special thanks to Dr Erica Smyth and Dr Roser Farre Garros for conducting assessment of cardiac section damage.

We thank the Medical Research Council (UK) and Imanova Ltd. for funding a CASE award (S.M.) and the Biotechnology and Biological Sciences Research Council (UK), GSK and Imanova Ltd. for funding a CASE award (A.H).

KEY POINTS

QUESTION: Is ^{18}F-Mitophos applicable to imaging mitochondrial dysfunction upon acute DOX cardiotoxicity?

PERTINENT FINDINGS: The pharmacokinetic profile of ^{18}F-Mitophos in rodents is suitable for cardiac imaging, with fast liver clearance a notable advantage over current in-human lipophilic cation tracers. Significant and dose responsive decrease in ^{18}F-Mitophos cardiac uptake was observed upon acute DOX treatment. ^{18}F-Mitophos shows promise as a cardiac imaging agent and warrants further investigation into cardiotoxicity applications.

IMPLICATIONS FOR PATIENT CARE: Early detection of cardiotoxicity may improve chemotherapy morbidity rates.

References

1. Siegel RL, Miller KD, Jemal A. Cancer statistics, 2016. *CA Cancer J Clin*. 2016;66(1):7-30.

2. Blum RH, Carter SK. Adriamycin. *Ann Intern Med*. 1974;80(2):249.

3. Bloom MW, Hamo CE, Cardinale D, et al. Cancer Therapy–Related Cardiac Dysfunction and Heart Failure. *Circ Hear Fail*. 2016;9(1):e002761.

4. Octavia Y, Tocchetti CG, Gabrielson KL, Janssens S, Crijns HJ, Moens AL. Doxorubicin-induced cardiomyopathy: From molecular mechanisms to therapeutic strategies. *J Mol Cell Cardiol*. 2012;52(6):1213-1225.

5. Lefrak EA, Pitha J, Rosenheim S, Gottlieb JA. A clinicopathologic analysis of adriamycin cardiotoxicity. *Cancer*. 1973;32(2):302-314.

6. Chatterjee K, Zhang J, Honbo N, Karliner JS. Doxorubicin cardiomyopathy. *Cardiology*. 2010;115(2):155-162.

7. Layard MW, Basa P, Davis HL, Hoff AL Von, Rozencweig M, Muggia FM. Risk Factors for Doxorubicin-lnduced Congestive Heart Failure. *Ann Intern Med*. 1979;91(5):710.

8. Cardinale D, Colombo A, Bacchiani G, et al. Early Detection of Anthracycline Cardiotoxicity and Improvement With Heart Failure Therapy Clinical Perspective. *Circulation*. 2015;131(22):1981-1988.

9. Kongbundansuk S, Hundley WG. Noninvasive Imaging of Cardiovascular Injury Related to the Treatment of Cancer. *JACC Cardiovasc Imaging*. 2014;7(8):824-838.

10. Jiji RS, Kramer CM, Salerno M. Non-invasive imaging and monitoring cardiotoxicity of cancer therapeutic drugs. *J Nucl Cardiol*. 2012;19(2):377-388.

11. Bennink RJ, van den Hoff MJ, van Hemert FJ, et al. Annexin V imaging of acute doxorubicin cardiotoxicity (apoptosis) in rats. *J Nucl Med*. 2004;45(5):842-848.

12. Inglese E, Leva L, Matheoud R, et al. Spatial and temporal heterogeneity of regional myocardial uptake in patients without heart disease under fasting conditions on repeated whole-body 18F-FDG PET/CT. *J Nucl Med*. 2007;48(10):1662-1669.

13. de Geus-Oei L-F, Mavinkurve-Groothuis AMC, Bellersen L, et al. Scintigraphic techniques for early detection of cancer treatment-induced cardiotoxicity. *J Nucl Med*. 2011;52(4):560-571.

14. Olmos RAV, Bokkel Huinink WW te., Hoeve RFA te., et al. Assessment of anthracycline-related myocardial adrenergic derangement by [123i]metaiodobenzylguanidine scintigraphy. *Eur J Cancer*. 1995;31(1):26-31.

15. Damiani RM, Moura DJ, Viau CM, Caceres RA, Henriques JAP, Saffi J. Pathways of cardiac toxicity: comparison between chemotherapeutic drugs doxorubicin and mitoxantrone. *Arch Toxicol*. 2016;90(9):2063-2076.

16. Renu K, V.G. A, P.B. TP, Arunachalam S. Molecular mechanism of doxorubicin-induced cardiomyopathy – An update. *Eur J Pharmacol*. 2018;818:241-253.

17. Mou T, Zhang X. Research Progress on 18F-Labeled Agents for Imaging of Myocardial Perfusion with Positron Emission Tomography. *Molecules*. 2017;22(4):562.

18. Safee ZM, Baark F, Waters ECT, et al. Detection of anthracycline-induced cardiotoxicity using perfusion-corrected 99mTc sestamibi SPECT. *Sci Rep*. 2019;9(1):216.

19. Haslop A, Gee A, Plisson C, Long N. Fully automated radiosynthesis of [1-(2-[18F]fluoroethyl),1H[1,2,3]triazole 4-ethylene] triphenylphosphonium bromide as a potential positron emission tomography tracer for imaging apoptosis. *J Label Compd Radiopharm*. 2013;56(6):313-316.

20. Haslop A, Wells L, Gee A, Plisson C, Long N. One-pot multi-tracer synthesis of novel (18)F-labeled PET imaging agents. *Mol Pharm*. 2014;11(11):3818-3822.

21. Ravert HT, Madar I, Dannals RF. Radiosynthesis of 3-[18F]fluoropropyl and 4-[18F]fluorobenzyl triarylphosphonium ions. *J Label Compd Radiopharm*. 2004;47(8):469-476.

22. Handley MG, Medina RA, Mariotti E, et al. Cardiac Hypoxia Imaging: Second-Generation Analogues of 64Cu-ATSM. *J Nucl Med*. 2014;55(3):488-494.

23. Mariotti E, Veronese M, Dunn JT, et al. Assessing radiotracer kinetics in the

Langendorff perfused heart. *EJNMMI Res*. 2013;3(1):74.

24. Poussios D, Andreadou I, Papalois A, et al. Protective effect of a novel antioxidant non-steroidal anti-inflammatory agent (compound IA) on intestinal viability after acute mesenteric ischemia and reperfusion. *Eur J Pharmacol*. 2003;465(3):275-280.

25. Erboga M, Bozdemir Donmez Y, Sener U, Fidanol Erboga Z, Aktas C, Kanter M. Effect of Urtica Dioica against Doxorubicin-Induced Cardiotoxicity in Rats through Suppression of Histological Damage, Oxidative Stress and Lipid Peroxidation. *Eur J Gen Med*. 2016;13(2):139-144.

26. Zhang X, Liu XJ, Wu Q, et al. Clinical outcome of patients with previous myocardial infarction and left ventricular dysfunction assessed with myocardial (99m)Tc-MIBI SPECT and (18)F-FDG PET. *J Nucl Med*. 2001;42(8):1166-1173.

27. DePuey, Gordon; Rozanski A. Using Gated Technetium-99m-Sestamibi SPECT to Characterize Fixed Myocardial Defects as Infarct or Artifact. *J Nucl Med*. 1993;34(34):952-955.

28. Madar I, Ravert H, DiPaula A, Du Y, Dannals RF, Becker L. Assessment of Severity of Coronary Artery Stenosis in a Canine Model Using the PET Agent 18F-Fluorobenzyl Triphenyl Phosphonium: Comparison with 99mTc-Tetrofosmin. *J Nucl Med*. 2007;48(6):1021-1030.

29. Shoup TM, Elmaleh DR, Brownell A-L, Zhu A, Guerrero JL, Fischman AJ.

Evaluation of (4-[18F]Fluorophenyl)triphenylphosphonium Ion. A Potential Myocardial Blood Flow Agent for PET. *Mol Imaging Biol*. 2011;13(3):511-517.

30. Madar I, Ravert H, Nelkin B, et al. Characterization of membrane potential-dependent uptake of the novel PET tracer 18F-fluorobenzyl triphenylphosphonium cation. *Eur J Nucl Med Mol Imaging*. 2007;34(12):2057-2065.

31. Srinivasan S, Muhammad C, Ravert H, et al. Human biodistribution and radiation dosimetry of 18F-fluorobenzyltriphenyl phosphonium. *J Nucl Med*. 2012;53(supplement 1):1512.

32. Kwatra M, Kumar V, Jangra A, et al. Ameliorative effect of naringin against doxorubicin-induced acute cardiac toxicity in rats. *Pharm Biol*. 2016;54(4):637-647.

33. Goyal SN, Mahajan UB, Chandrayan G, et al. Protective effect of oleanolic acid on oxidative injury and cellular abnormalities in doxorubicin induced cardiac toxicity in rats. *Am J Transl Res*. 2016;8(1):60-69.

34. Saad SY, Najjar TA, Al-Rikabi AC. The preventive role of deferoxamine against acute doxorubicin-induced cardiac, renal and hepatic toxicity in rats. *Pharmacol Res*. 2001;43(3):211-218.

35. Ferreira de Souza T, Quinaglia A.C. Silva T, Osorio Costa F, et al. Anthracycline Therapy Is Associated With Cardiomyocyte Atrophy and Preclinical

Manifestations of Heart Disease. *JACC Cardiovasc Imaging*. 2018;11(8):1045-1055.

36. Willis MS, Parry TL, Brown DI, et al. Doxorubicin Exposure Causes Subacute Cardiac Atrophy Dependent on the Striated Muscle–Specific Ubiquitin Ligase MuRF1. *Circ Hear Fail*. 2019;12(3).

TABLE 1

^{18}F-FBnTP	**5**	**15**	**30**	**60**
Blood	0.12 (0.22)	0.16 (0.06)	0.12 (0.06)	0.04 (0.01)
Plasma	0.56 (0.51)	0.08 (0.06)	0.05 (0.04)	0.02 (0.00)
Muscle	0.30 (0.12)	0.22 (0.12)	0.21 (0.04)	0.34 (0.14)
Spleen	5.63 (0.28)	4.58 (1.22)	3.17 (1.65)	2.49 (0.76)
Liver	3.71 (0.93)	3.57 (0.65)	3.58 (1.06)	3.59 (0.73)
Adrenals	6.87 (9.16)	9.84 (1.74)	11.33 (5.33)	7.00 (2.49)
Kidney	17.57 (5.27)	30.08 (3.81)	32.24 (3.44)	25.81 (5.92)
Lung	2.09 (0.38)	2.03 (0.12)	2.09 (0.27)	1.63 (0.47)
Heart	7.42 (0.43)	7.32 (0.69)	7.93 (2.45)	6.75 (1.54)
Brain	0.07 (0.03)	0.05 (0.01)	0.06 (0.02)	0.03 (0.01)
Heart/Plasma	13.2 (12.0)	95.6 (70.9)	153.1 (135.2)	422.7 (142.5)
Heart/Lung	3.6 (0.7)	3.6 (0.4)	3.8 (1.3)	4.1 (1.5)
Heart/Liver	2.0 (0.5)	2.1 (0.4)	2.2 (0.9)	1.9 (0.6)
^{18}F-Mitophos	**5**	**15**	**30**	**60**
Blood	0.35 (0.17)	0.16 (0.02)	0.14 (0.02)	0.06 (0.02)
Plasma	0.19 (0.11)	0.06 (0.01)	0.07 (0.02)	0.02 (0.01)
Muscle	0.30 (0.04)	0.22 (0.02)	0.24 (0.06)	0.22 (0.06)
Spleen	6.67 (1.87)	6.04 (0.36)	7.28 (0.55)	4.231 (0.83)
Liver	3.91 (0.69)	2.25 (0.30)	1.53 (0.30)	0.463 (0.12)
Adrenals	12.50 (4.52)	11.32 (1.31)	21.16 (6.47)	14.30 (4.25)
Kidney	20.77 (1.63)	17.76 (0.28)	21.69 (1.37)	18.64 (4.57)
Lung	2.36 (0.15)	2.97 (1.42)	1.43 (0.25)	1.37 (0.36)
Heart	5.40 (0.61)	4.60 (0.32)	5.17 (0.56)	5.17 (0.86)
Brain	0.08 (0.01)	0.07 (0.00)	0.06 (0.01)	0.05 (0.01)
Heart /Plasma	28.3 (16.6)	82.2 (15.7)	95.7 (36.9)	303.9 (185.8)
Heart /Lung	2.3 (0.3)	1.6 (0.7)	3.6 (0.7)	3.8 (0.6)
Heart /Liver	1.4 (0.5)	2.0 (0.2)	3.4 (0.8)	11.2 (1.2)

Selected *ex vivo* biodistribution data for ^{18}F-FBnTP and ^{18}F-Mitophos and heart to tissue ratios for selected tissues. All values are reported as average SUV (SD) determined by gamma counter measurement for each timepoint/ min.

TABLE 2

	Assessor 1		Assessor 2	
Dose	Average median	Range	Average median	Range
Control	0	0-1	0.5	0-2
10 mg/kg	2	0-3	2.5	0-3
15 mg/kg	2.5	1-3	2.75	2-3
20 mg/kg	2.25	1-3	2.5	1-3

Histological assessment of H&E stained tissue sections of control and DOX treated myocardium. Each section was scored with severity rating of 0 (NAD), 1 (mild signs of damage), 2 (moderate), or 3 (severe). The average median donates the median score of each heart (n = 3 sections) averaged over the treatment group. The range denotes the total range of sections within a treatment group.

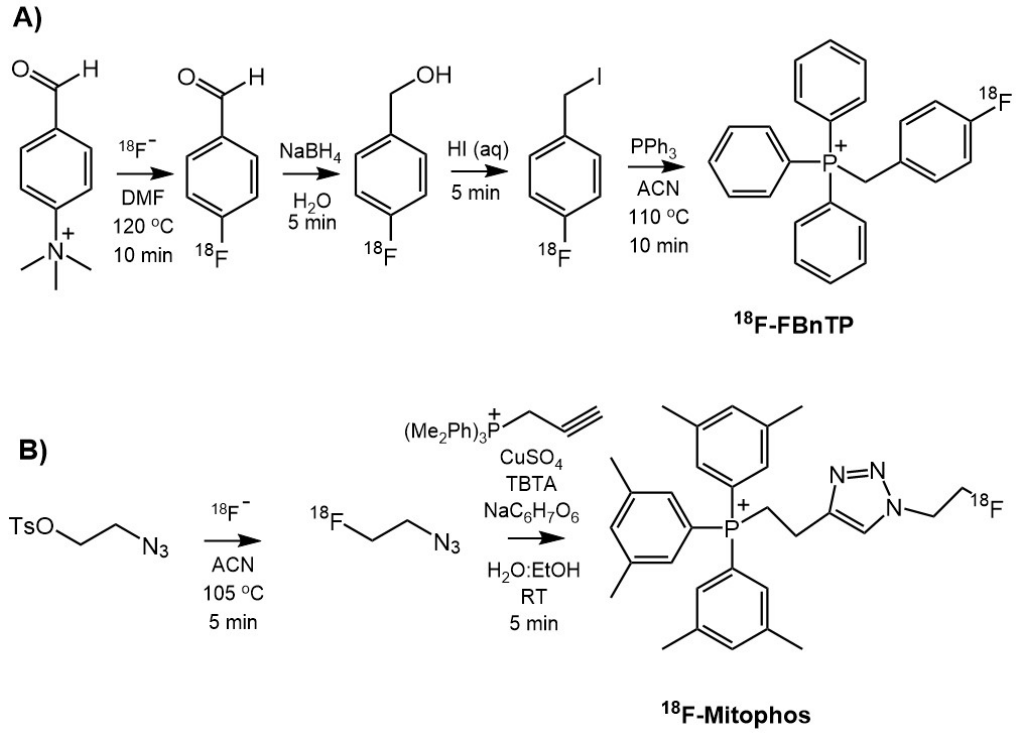

FIGURE 1. Radiosynthetic pathway for PET tracers. A) ^{18}F-FBnTP B) ^{18}F-Mitophos. TBTA is tris(benzyltriazolylmethyl)amine, RT is room temperature and $NaC_6H_7O_6$ is sodium ascorbate.

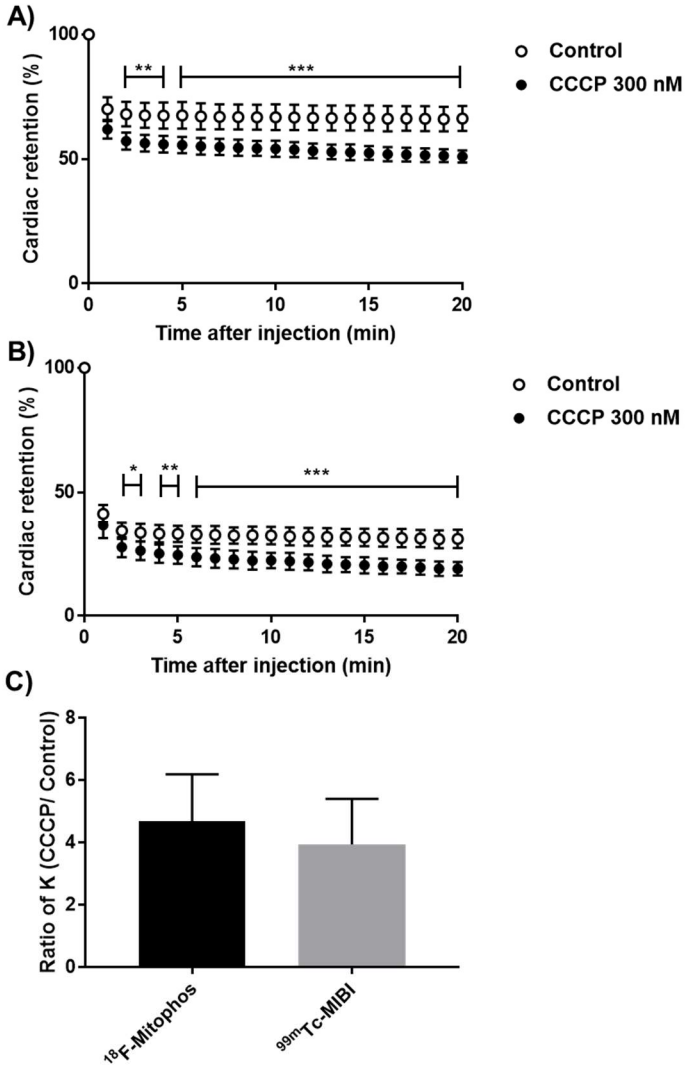

FIGURE 2. Cardiac retention of percentage injected dose of A) ^{18}F-Mitophos and B) ^{99m}Tc- Sestamibi in Langendorff perfused hearts in control and CCCP (300 nM) treated. C) Relative increase in washout rate, K, (CCCP treated/control) hearts for ^{18}F-Mitophos and ^{99m}Tc-Sestamibi. (Statistical analysis was two-way ANOVA and Dunnett's post hoc analysis (A, B) and two tailed t-test (C). * $P< 0.05$, ** $P< 0.01$, *** $P< 0.001$).

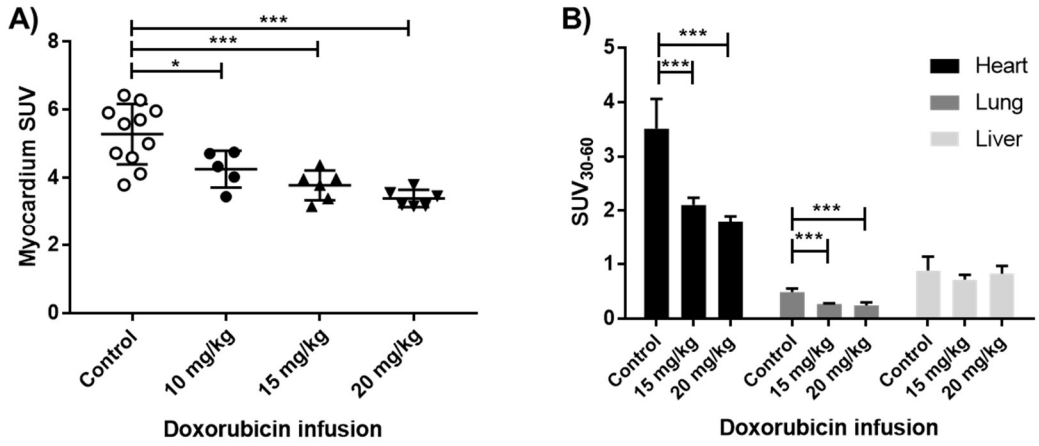

FIGURE 3. Uptake of ^{18}F-Mitophos in control and DOX treated animals (mean ± SD). A) *Ex vivo* biodistribution of collected cardiac tissue (60 min p.i.). B) Average $SUV_{30\text{-}60}$ from left ventricle, lung and liver TAC, derived from dynamic PET-CT scan. (Statistical analysis was one-way ANOVA and Dunnett's *post hoc* analysis. * P<0.05, *** P<0.001).

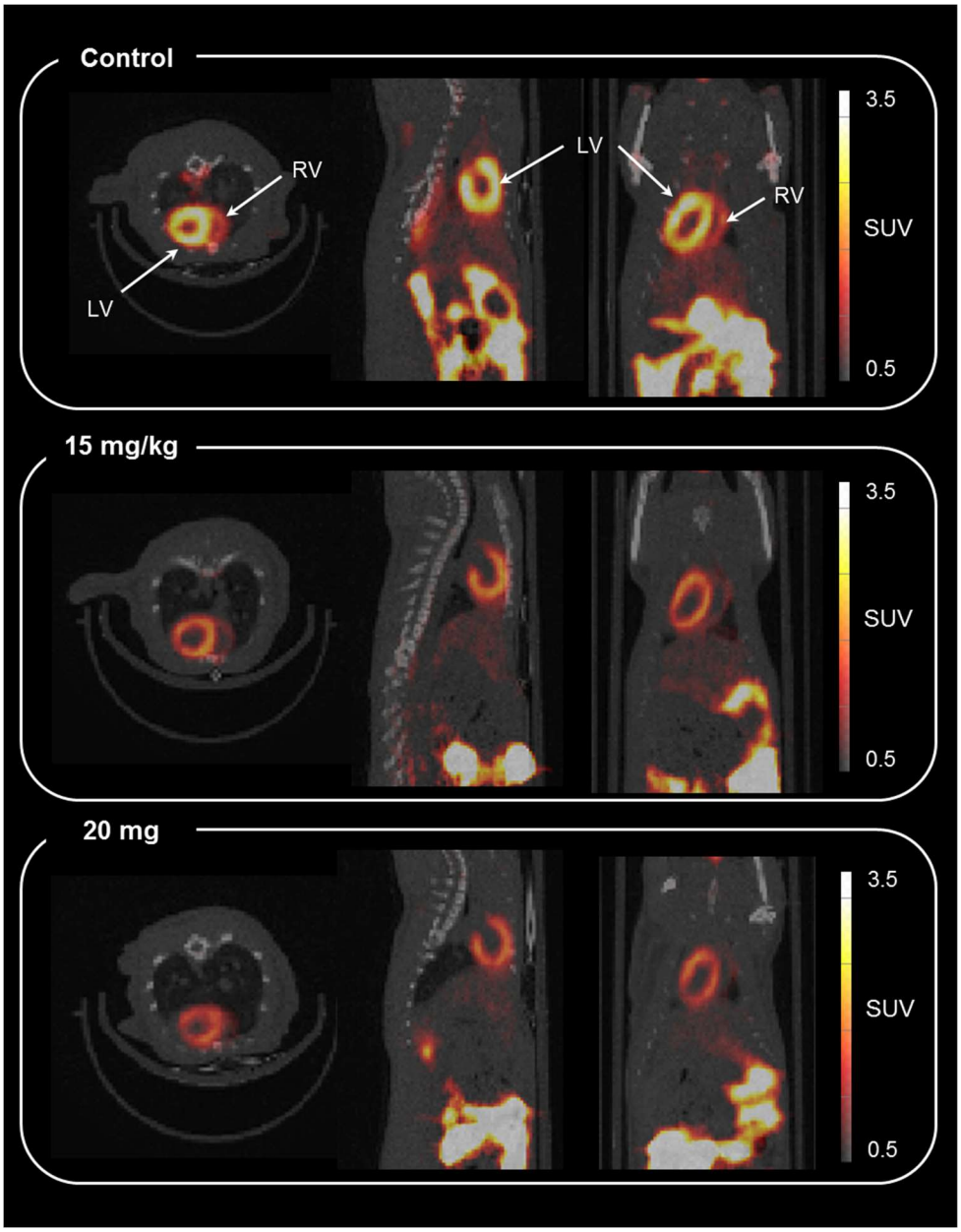

FIGURE 4. Representative axial, sagittal and coronal co-registered PET-CT image (summed from 30 to 60 min) ^{18}F-Mitophos in Sprague Dawley rats 48 h post DOX dose. Control (top), 15 mg/kg (middle) and 20 mg/kg (bottom). The left and right ventricles are highlighted with LV and RV respectively.

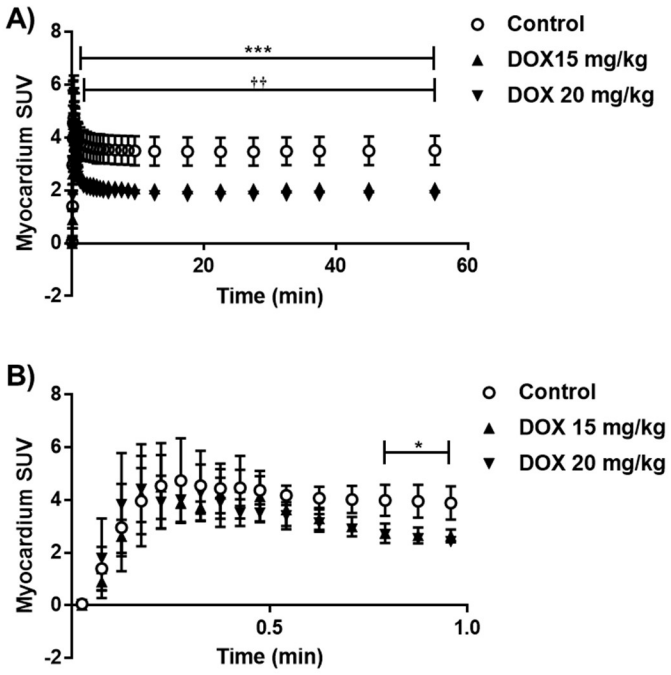

FIGURE 5. TACs (average SUV ± SD) of ^{18}F-Mitophos in Sprague Dawley rats for the left ventricle. SUV's are displayed over the duration of the scan (A) and for the first minute (B). Significant decrease in cardiac uptake for both the 15 mg/kg and 20 mg/kg dose in the myocardium is observed. Statistical analysis two-way ANOVA and Dunnett's *post hoc* analysis. *** $P<0.001$ for control compared to DOX 20 mg/kg, †† $P<0.01$ for control compared to DOX 15 mg/kg *, ** and † confidence intervals were omitted for clarity in A) and occurred only prior indicated regions.

Online Supplement: Imaging chemotherapy induced acute cardiotoxicity with lipophilic cation ^{18}F-Mitophos

Methods and Materials

Radiochemistry Procedures

Production of ^{18}F-FBnTP

To ^{18}F-fluoride, azeotropically dried in the presence of Kryptofix and K_2CO_3, 4-trimethylammoniumbenzaldehyde (10 mg) in dimethylformamide (DMF, 400 µL) was added, and heated to 110 °C for 10 min. Sodium borohydrate (15 mg) in H_2O (500 µL) was added to the cooled reaction vessel and reacted at room temperature for 5 min. Conc. hydroiodic acid (1 mL) was added to the same reaction vial and reacted for 10 min. The reaction mixture was diluted with H_2O and passed through a C-18 cartridge. The cartridge was washed with sodium thiosulphate/K_2CO_3 solution and water before elution with ACN through molecular sieves and a sodium sulphate drying cartridge, into a vial containing triphenyl phosphine (21 mg) in ACN (Figure. 1). The sealed vial was heated to 110 °C for 10 min before being allowed to cool to room temperature. ^{18}F-FBnTP was then purified by HPLC and reformulated in 10 % ethanol, saline solution. Purity was confirmed by analytical radio-HPLC. Specific activity 15.0 ± 12.6 GBq/µmol.

Production of ^{18}F-Mitophos

Tosyl ethyl azide in acetonitrile (ACN) was added to ^{18}F-fluoride, azeotropically dried in the presence of Kryptofix and K_2CO_3, and heated for 5 min at 105 °C. ^{18}F-Fluoroethyl azide was distilled into a vial containing $CuSO_4 \cdot 5H_2O$ (56 µL, 0.4 mmol/L), tris(benzyltriazolylmethyl)amine (TBTA) (1 mg), sodium ascorbate (40 mg) 3-but-3-ynyl (tris-3,5-dimethylphenyl)phosphonium bromide (2 mg) in H_2O:EtOH 3:1

solution. The reaction was left for 5 min after distillation had completed and reaction mixture purified by isocratic high performance liquid chromatography (HPLC) (ACN: ammonium formate buffer, pH 4 100 mmol/L, 50:50) (Figure. 1). ^{18}F-Mitophos was reformulated in 10 % EtOH and saline and purity confirmed by analytical radio-HPLC. Specific activity 24.6 ± 18.3 GBq/µmol.

Animal Procedures

Animal husbandry

Animals were group-housed within individually ventilated cages with Aspen grade 6 bedding under a 12/12 light dark cycle (lights on 7am, off 7pm) at set temperature and humidity ranges of 19-23 °C and 45-65 % respectively. Food and water were available *ad libitum* and environmental enrichment was provided.

Langendorff Heart Perfusion

After intraperitoneal injection of pentobarbital, hearts were excised from male Wistar rats and cannulated onto a Langendorff perfusion rig. Hearts were perfused with modified Krebs-Henseleit buffer (37°C gassed with 95 % O_2/ 5 % CO_2) at a constant flow rate of 14 mL/min. Cardiac tracer retention and washout was monitored throughout each experiment using GinaSTAR software via the triple γ-detection system, while cardiac contractile function was monitored with an intraventricular balloon connected to a Powerlab system running Labchart software (AD Instruments Ltd). After a stabilisation period of 20 min, CCCP (at a final concentration of 300 nmol/L) or vehicle was infused into the aortic cannula via a side arm. After 25 min, a bolus of radiotracer (approximately 1 MBq, 50-100 µl) was injected into the arterial line.

In vivo procedures

All *in vivo* and procedures were carried out under anaesthesia (2-3 % isoflurane in air 1 L/min) and animal body temperature maintained by heating mats, with rectal probe feedback. For dynamic PET:CT cardiac scanning, animals were placed within the central bore of a Siemens Inveon PET-CT scanner with the field of view over the heart. A CT scan was conducted for attenuation correction before injection of radiotracer and dynamic PET data acquired (60 min). Radiopharmaceuticals were administered via direct venepuncture of the tail vein. At the end of the protocol animals were culled via exsanguination under deep anaesthesia (4 % isoflurane, air 1L/min) and tissues were collected in ice-cold saline, weighed and radioactivity measured via gamma counter (Wizard). Dynamic scan data was histogrammed (frames, sec; 10, 3; 6, 5; 8, 30; 5, 60; 6, 300; 2, 600) and reconstructed (2D-filter back projection). One animal within the DOX study was excluded due to a failed IV injection and was part of the 10 mg/kg group, this data point was not replaced.

***Ex vivo* analysis**

Metabolite quantification

Blood samples were periodically collected (5, 10, 20, 40 and 60 min, n=3 per timepoint). Proteins were precipitated from plasma with acetonitrile (ACN) (1:1) and centrifugation at 12000 x g for 5 min 90 % ACN: 10 % 50 mM ammonium formate, pH 4, 5 mL/min, was used as the mobile phase with a Phenomenex Prodigy semi-preparative column ODS(3), (10 micron, 250 x 10 mm) column. Typical activity recovery from HPLC was >90 %.

Malondialdehyde (MDA) quantification

Left ventricle tissue from the apex of the heart was homogenised in ice cold 20 mM Tris-HCL buffer pH 7.4 in a 1:10 ratio before briefly sonicating samples. Homogenate was centrifuged at 3000 x g for 10 min at 4 °C and the supernatant removed for analysis 200 μL of tissue homogenate was added to 650 μL of

10.3 mmol/L *N*-methyl-2-phenyl-indole in ACN and vortexed for 3-4 s. 150 μL of HCL 37 % was added and samples incubated at 45 °C for 60 min. The samples were cooled in ice and centrifuged before 3 x 200 μL aliquots per sample were transferred to a 96 well plate for reading (absorbance, 586 nm). A standard curve from 1.25 to 40 nmol/mL MDA was used for quantification (R^2 >0.999).

Target Organ	Alpha	Beta	Photon	Total	EDE Cont.	ED Cont.
Adrenals	0.00E+00	7.40E-02	1.95E-02	9.34E-02	5.61E-03	2.34E-04
Brain	0.00E+00	2.94E-04	2.17E-03	2.46E-03	0.00E+00	6.15E-06
Breasts	0.00E+00	8.89E-04	3.60E-03	4.49E-03	6.74E-04	2.25E-04
Gallbladder Wall	0.00E+00	8.89E-04	1.81E-02	1.90E-02	0.00E+00	0.00E+00
LLI Wall	0.00E+00	7.88E-03	2.11E-02	2.90E-02	0.00E+00	3.47E-03
Small Intestine	0.00E+00	1.53E-01	3.77E-02	1.91E-01	1.14E-02	4.77E-04
Stomach Wall	0.00E+00	*2.29E-02*	1.64E-02	*3.93E-02*	0.00E+00	*4.71E-03*
ULI Wall	0.00E+00	1.08E-02	4.06E-02	5.14E-02	3.09E-03	1.29E-04
Heart Wall	0.00E+00	2.38E-02	1.12E-02	3.50E-02	0.00E+00	0.00E+00
Kidneys	0.00E+00	9.37E-02	3.85E-02	1.32E-01	7.93E-03	3.30E-03
Liver	0.00E+00	4.87E-03	1.08E-02	1.56E-02	0.00E+00	7.81E-04
Lungs	0.00E+00	8.11E-03	6.33E-03	1.44E-02	1.73E-03	1.73E-03
Muscle	0.00E+00	1.19E-03	7.27E-03	8.46E-03	0.00E+00	2.11E-05
Ovaries	0.00E+00	8.89E-04	2.74E-02	2.83E-02	7.08E-03	5.66E-03
Pancreas	0.00E+00	2.80E-03	1.42E-02	1.70E-02	0.00E+00	4.24E-05
Red Marrow	0.00E+00	5.45E-03	1.12E-02	1.66E-02	2.00E-03	2.00E-03
Osteogenic Cells	0.00E+00	1.79E-02	7.92E-03	2.58E-02	7.75E-04	2.58E-04
Skin	0.00E+00	8.89E-04	3.64E-03	4.52E-03	0.00E+00	4.52E-05
Spleen	0.00E+00	2.75E-02	1.95E-02	4.70E-02	0.00E+00	1.18E-04
Testes	0.00E+00	8.89E-04	4.68E-03	5.57E-03	0.00E+00	0.00E+00
Thymus	0.00E+00	3.32E-03	4.96E-03	8.27E-03	0.00E+00	2.07E-05
Thyroid	0.00E+00	8.78E-02	1.58E-02	1.04E-01	3.11E-03	5.18E-03
Urinary Bladder Wall	0.00E+00	3.72E-02	2.40E-02	6.13E-02	3.68E-03	3.06E-03
Uterus	0.00E+00	8.89E-04	2.59E-02	2.68E-02	0.00E+00	6.70E-05
Total Body	0.00E+00	4.34E-03	7.99E-03	1.23E-02	0.00E+00	0.00E+00
Effective Dose Equivalent (mSv/MBq)					**4.71E-02**	
Effective Dose (mSv/MBq)						**3.15E-02**

SUPPLEMENT TABLE. 1. Dosimetry data for ^{18}F-Mitphos calculated from Sprague Dawley rats (n=3 per timepoint at 5, 15, 30 and 60 min).

Clinical sign	**10 mg/kg**	**15 mg/ kg**	**20 mg/kg**
Piloerection	3/6	5/6	6/6
Hunched posture	1/6	1/6	2/6
Vocalisation	0/6	1/6	0/6
Average BW loss/ %	5.3 ± 2.8	7.0 ± 1.5	6.5 ± 2.4

SUPPLEMENT TABLE. 2. Adverse effects signs observed for DOX infused animals over the 48 h period post dose. Animals were assessed twice daily and weighed daily. Weight loss is quoted as the total weight loss over the 48 h period.

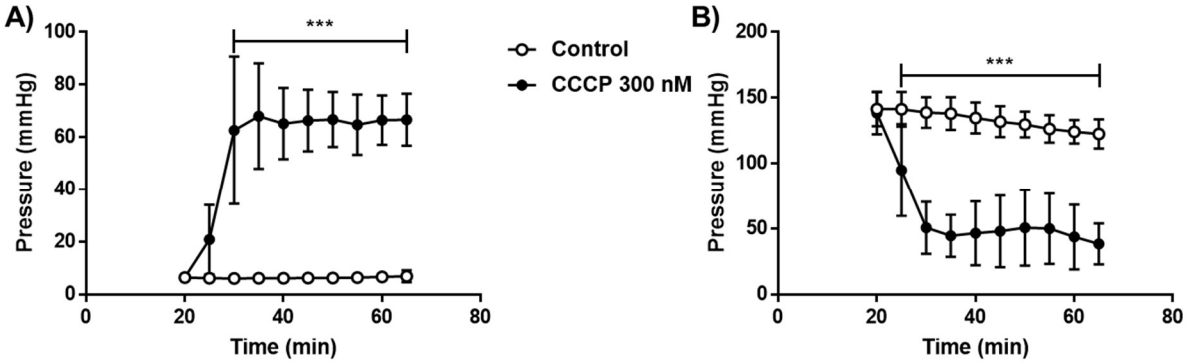

SUPPLEMENT FIGURE. 1. Cardiac parameters for hearts perfused on the Langendorff perfusion rig. Significant response to both A) LVEDP and B) LVDP are observed upon treatment with CCCP 300 nM from 20 min until the end of protocol showing decreased function of the perfused heart upon CCCP infusion. Data prior to 20 min represents manual perfusion of the heart and stabilisitation period and is therefore excluded. Statistical analysis was 2-way ANOVA and Dunnett's post hoc analysis. *** $P<0.001$.

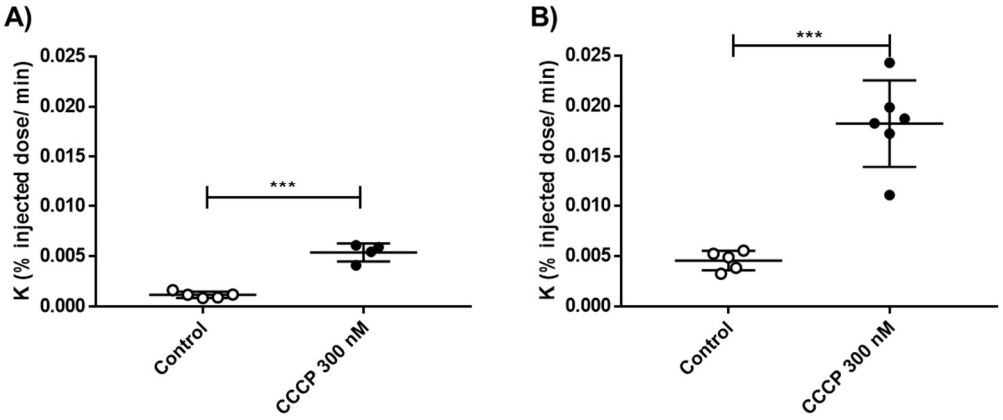

SUPPLEMENT FIGURE. 2. Washout rate, K, in the Langendorff perfused heart model. K is the least square fit of the exponential washout rate between 2 min post injection and 20 min post injection for A) ^{18}F-Mitophos and B) ^{99m}Tc-Sestamibi. Statistical analysis was 1-tailed student t-test, *** P<0.001.

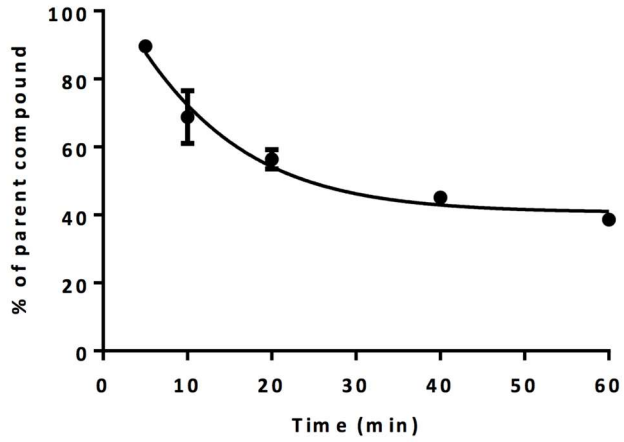

SUPPLEMENT FIGURE. 3. Metabolism profile of ^{18}F-Mitophos in Sprague Dawley rats (n=2). Plasma was extracted from blood samples and compared to metabolite concentrations via HPLC chromatogram. >90 % activity was recovered from HPLC.

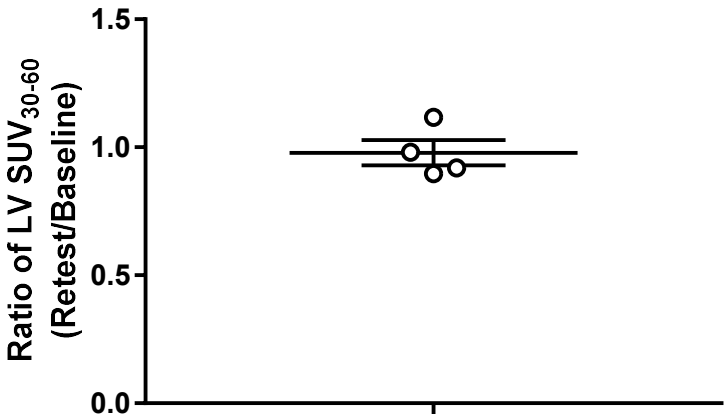

SUPPLEMENT FIGURE. 4. Test-retest data of ^{18}F-Mitophos uptake in cardiac tissue at 60 min in Sprague Dawley rats. Ratio of left ventricle SUV_{30-60} derived from dynamic scan TAC's (retest/baseline) from two scans 48-72 h apart was used.

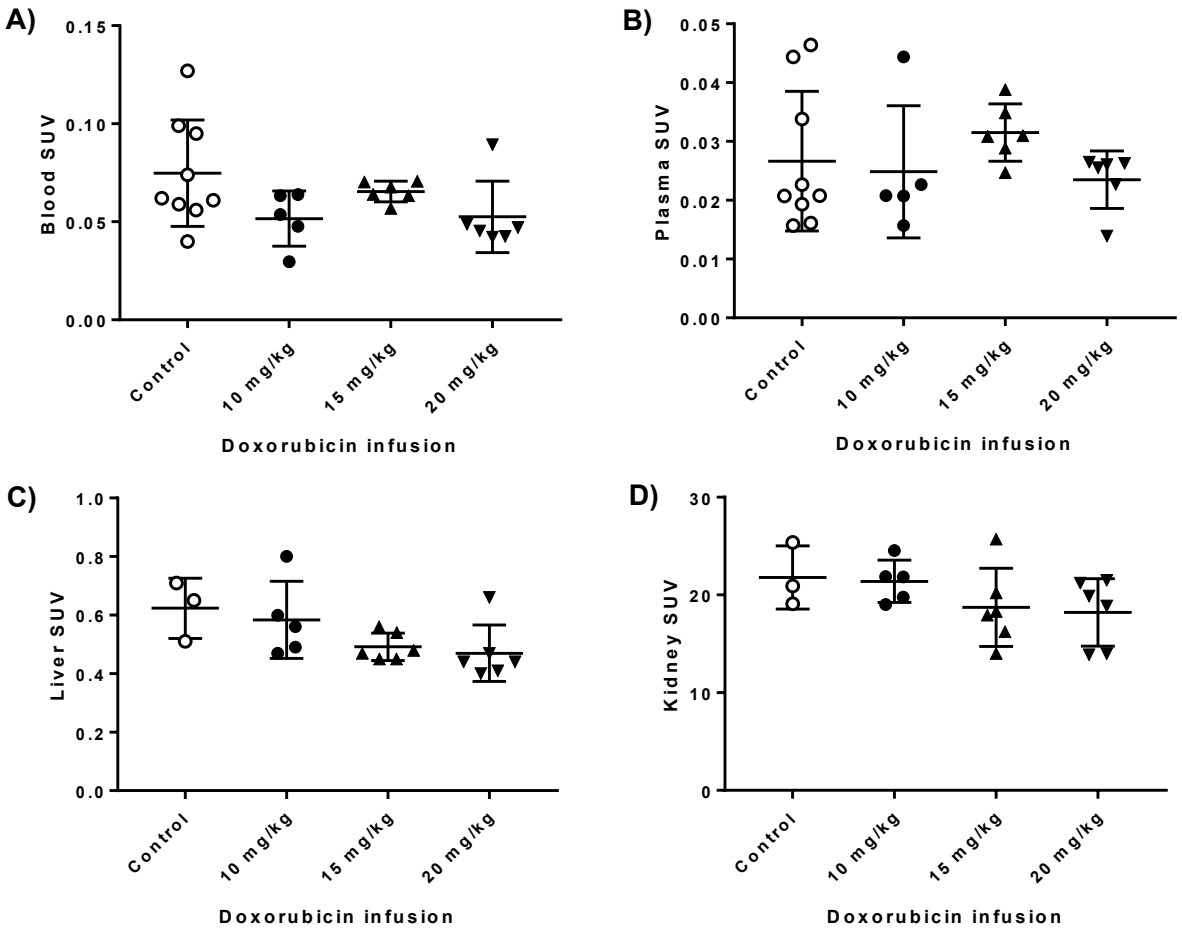

SUPPLEMENT FIGURE. 5. Cut and count activity at 60 min p.i. of ^{18}F-Mitophos in blood (A), plasma (B), Liver (C) and kidney (D) from control and DOX treated rats. No significant alteration was observed in any tissue group.

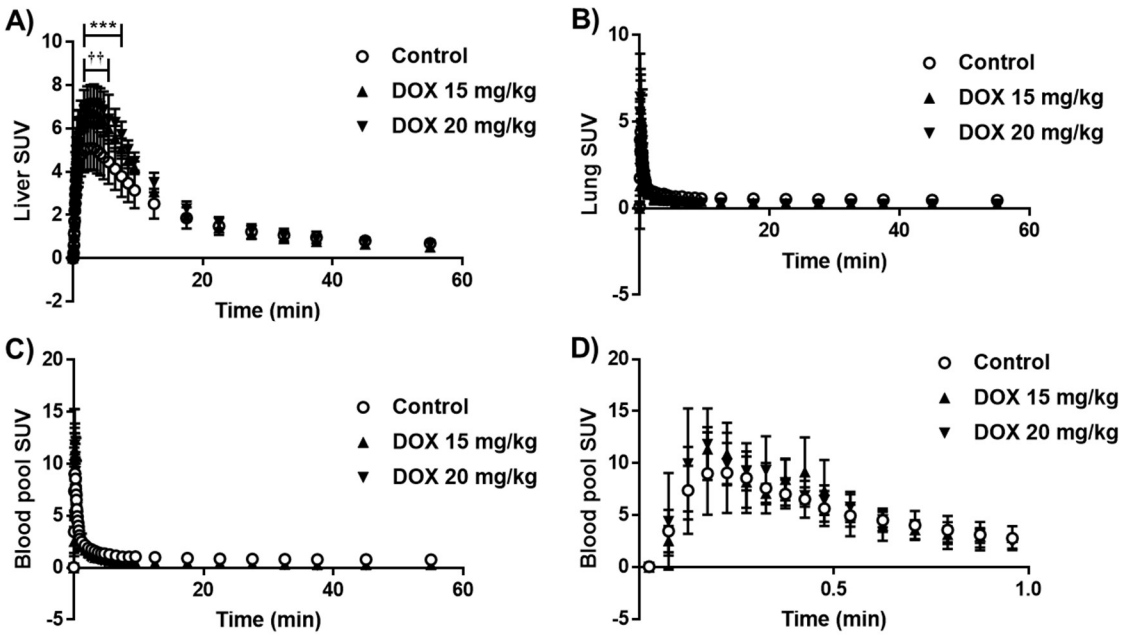

SUPPLEMENT FIGURE. 6. Time activity curves (average SUV ± SD) of ^{18}F-Mitophos in Sprague Dawley rats from A) liver, B) lung, C) blood pool and D) blood pool from the first minute. *** P<0.001 for control compared to DOX 20 mg/kg, †† P<0.01 for control compared to DOX 15 mg/kg *, ** and † confidence intervals were omitted for clarity in A) and occurred only directly adjacent to indicated regions. Blood pool TAC after approximately 1 min must be treated with extreme caution as, due to the proximity and SUV differences to the myocardium, large partial volume effect is observed.

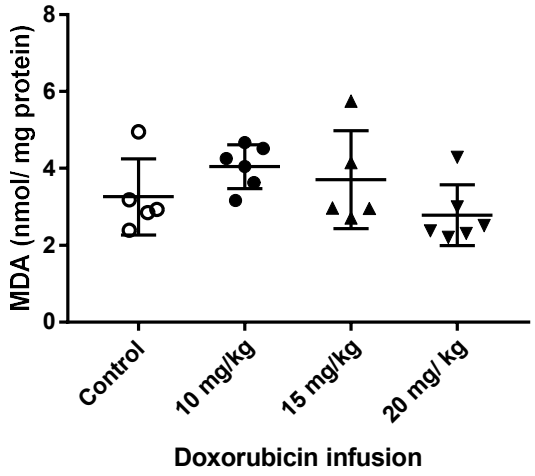

SUPPLEMENT FIGURE. 7. MDA levels measured in the apex of the cardiac tissue from control and DOX treated groups.

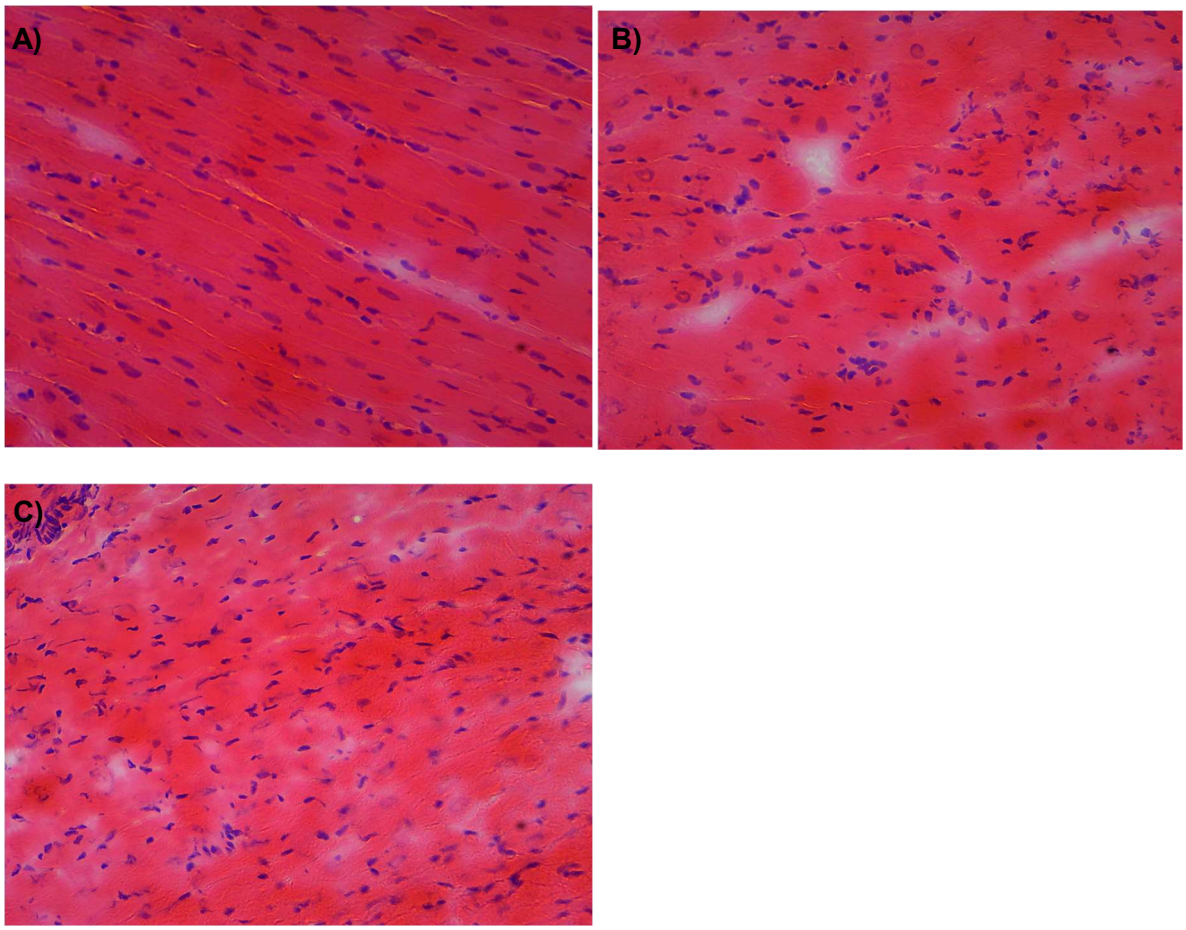

SUPPLEMENT FIGURE. 8. Example H&E stained longitudinal left ventricle sections (10 µm). A) control tissue, B) moderate damage, C) severe damage. Sections were assessed for myofibrillar loss, cytoplasmic vacuolisation, myocardial disorganisation, inflammatory cell infiltration and haemorrhages.